

An analysis of supercritical adsorption in the context of continuum mechanics

Kaibin Fu^a, Richard L. Robinson^b, John C. Slattery^{a,*}

^aDepartment of Aerospace Engineering, Texas A&M University, College Station, TX 77843-3141, USA

^bDepartment of Chemical Engineering, Zachry Engineering Center, Texas A&M University, College Station, TX 77843-3122, USA

Received 17 March 2002; accepted 14 September 2003

Abstract

To illustrate a new extension of continuum mechanics to the nanoscale (not the molecular scale), we analyze the supercritical adsorption of argon, krypton, and methane on Graphon. We compare our results both with existing experimental data and with prior molecular-based theories.

© 2003 Published by Elsevier Ltd.

Keywords: Adsorption; Argon; Films; Interface; Krypton; Methane; Nanoscale; Supercritical fluid

1. Introduction

Far from a solid–fluid interface on a molecular scale, the density of a gas, either subcritical or supercritical, approaches the bulk density. Within a few molecular diameters of the interface, the gas is subjected to intense attractive intermolecular forces attributable to the solid. The magnitudes of these forces increase as the distance to the interface decreases. With a subcritical gas or vapor, condensation occurs. With a supercritical fluid, the density increases as the interface is approached, becoming similar to that of a liquid. We will confine our attention here to the case of a supercritical fluid. We explore the “adsorption” or densification of three supercritical gases on Graphon: argon, krypton, and methane.

Specovius and Findenegg (1978) used a gravimetric method for the determination of surface excess isotherms of argon and methane on Graphon (a graphitized carbon black) for temperatures from -20°C to 50°C and pressures up to 150 bar. This corresponded to bulk densities up to the critical density for methane and more than half the critical density for argon. Blumel et al. (1982) performed a similar study for krypton on Graphon but for temperatures up to 100°C .

Five analyses of these data starting from a molecular point of view have been published.

- Egorov (2001) presented a microscopic statistical mechanical theory of adsorption of supercritical fluids. The theory is in excellent agreement with the experimental observations of Specovius and Findenegg (1978) and Blumel et al. (1982) for argon and krypton, although the error increases at higher densities as the temperature approaches the critical temperature.
- Rangarajan et al. (1995) developed a mean-field model that superimposes the fluid–solid potential on a fluid equation of state to predict adsorption on a flat wall. Their paper shows some predicted adsorption isotherms for krypton but none for argon or methane.
- Sokolowski (1982) used the Percus–Yevick equation for the local density of a gas in contact with a flat solid surface to calculate the adsorption characteristics of argon and of methane on graphite. The calculations used the Boltzmann-averaged potential (Abraham and Singh, 1978), which is calculated from the particle–graphite basal-plane potential (Steele, 1973), for the gas–surface interaction and used the Lennard–Jones (12,6) potential for the gas–gas interactions.
- Fischer (1978) used a model for high-temperature and high-pressure adsorption that was the same as the one introduced in previous papers (Fischer, 1977; Findenegg and Fischer, 1975) for moderate pressures. He assumed

* Corresponding author. Department of Chemical Engineering, Zachry Engineering Center, Texas A&M University, College Station, TX 77843-3122, USA. Tel.: 01-979-845-0407; fax: +1-979-845-6051.

E-mail address: slattery@tamu.edu (J.C. Slattery).

that a hard sphere gas was in contact with a structureless plane wall and that a Lennard–Jones potential described the wall–particle interaction.

- Aranovich and Donohue (1996) used two adjustable parameters in comparing the Ono and Kondo (1960) theory to the data reported by Specovius and Findenegg (1978).

The first four of these analyses will be discussed further in Section 5.

There have been a number of studies of supercritical adsorption on activated carbons, both theoretical and experimental (Gusev et al., 1997; Neimark and Ravikovitch, 1997; Miyawaki et al., 1998; Zhou et al., 2000; Murata and Kaneko, 2001; Cao et al., 2002; Lozano-Castelló et al., 2002; Ohkubo et al., 2002). While activated carbons are of immense practical importance, they are not well-suited to test theories, because they are porous and the effects of intermolecular forces are more complex. For this reason, they will not be discussed here.

The purpose of this paper is to present the first and simplest application of a new extension of continuum mechanics to the nanoscale (not the molecular scale). Specifically, in the immediate neighborhood of phase interfaces, we introduce a body force representing a correction for intermolecular forces attributable to the adjoining phase.

Our intention here is not to find fault with prior analyses. Nor are we arguing that continuum mechanics is superior to a molecular point of view. To the extent that our approach may appear to have some advantages in describing experimental data, it must be kept in mind that we will be taking advantage of empirical equations of state for bulk behavior that the molecular-based theories do not use.

2. Corrections for intermolecular forces

Surface excess variables such as the surface mass density, surface velocity, surface stress tensor, etc. account for changes in the corresponding quantities in the adjoining phases within the immediate neighborhood of the dividing surface (Slattery, 1990, Sections 1.3.2 and 2.1.8). These changes occur, because the behaviors of the two materials change as the dividing surface is approached.

Why is material behavior different in the interfacial region? All descriptions of material behavior at some distance from the interface are based upon the assumption that the material extends to “infinity” (perhaps 100 nm) in all directions. Material points outside the immediate neighborhood of the interface are subjected to intermolecular forces only from one phase. Material points within the interfacial region are subjected to intermolecular forces from both phases.

Our premise is that material behavior within the interfacial region can be represented as bulk material behavior corrected for the intermolecular forces from the adjoining phase. In particular, we recognize the equivalence of stresses and body forces (Truesdell and Toupin, 1960, p. 549).

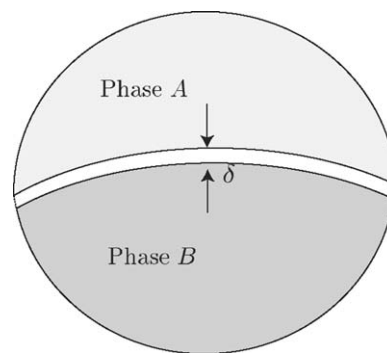


Fig. 1. A material body consisting of two adjoining phases, *A* and *B*.

There are three descriptions of the interfacial region of a single interface (as opposed to a thin film), each view having its own somewhat different notation.

- (a) Material behavior is a function of position within the interfacial region. No excess quantities are associated with any dividing surface. The problem with this view is that in general we will not know the appropriate descriptions of behavior in the interfacial regions.
- (b) In the second view, we use the descriptions of material behavior appropriate outside the interfacial region (bulk material behavior). The effects of the interfacial region are taken into account by the excess quantities assigned to the corresponding dividing surface (Slattery, 1990, Sections 1.3.5 and 2.1.6).
- (c) In the third view described in Fig. 1, we again use the descriptions of material behavior appropriate outside the interfacial region (bulk material behavior), corrected for intermolecular forces from the adjoining phase as described below. No excess properties are assigned to the dividing surface.

In the context of view (c), the differential and jump mass balances as well as the jump momentum balance take the usual forms (Slattery, 1999, p. 51 and 59). It is only the differential momentum balance that is changed, which for a static fluid becomes

$$-\nabla P^{(A)} + \mathbf{b}^{(A,\text{corr})} = 0. \quad (1)$$

Here P is thermodynamic pressure and $\mathbf{b}^{(A,\text{corr})}$ is the body force per unit volume attributable to the adjoining phase. Here and in what follows, we will neglect the effects of gravity.

Referring to Fig. 2, we reason that $\mathbf{b}^{(A,\text{corr})}$ represents the force per unit volume that results from

- subtracting the force per unit volume at a point in phase *A* attributable to that portion of phase *A* that has been replaced by phase *B*, and
- adding the force per unit volume at this same point in phase *A* attributable to phase *B*.

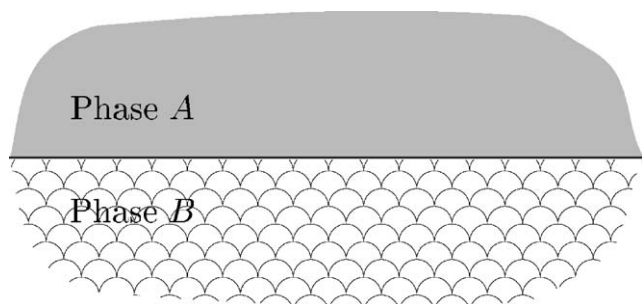


Fig. 2. Two semi-infinite phases *A* and *B* separated by a phase interface or dividing surface.

In other words, for each point in the gas phase *A*

$$\mathbf{b}^{(A,\text{corr})} \equiv - \int_{R^{(B)}} \mathbf{f}^{(A,A)} dV + \int_{R^{(B)}} \mathbf{f}^{(A,B)} dV. \quad (2)$$

Here $R^{(B)}$ is the region occupied by phase *B*, $\mathbf{f}^{(A,B)}(\mathbf{r}^{(A)}, \mathbf{r}^{(B)})$ is the force per unit volume of phase *A* per unit volume of phase *B* at a point $\mathbf{r}^{(A)}$ in phase *A* attributable to the material at point $\mathbf{r}^{(B)}$ in phase *B*, and dV indicates that a volume integration is to be performed.

In reality, the effective replacement region $R^{(B)}$ may be no more than 100 nm thick, since outside this region the intermolecular forces between phases *A* and *B* go to zero.

2.1. Estimating the two-point potential

The Lennard–Jones (6–12) potential is commonly recommended for non-polar dilute gases (Hirschfelder et al., 1954, p. 22)

$$\phi^{(A,B)} = 4\epsilon^{(A,B)} \left[\left(\frac{\sigma^{(A,B)}}{r} \right)^{12} - \left(\frac{\sigma^{(A,B)}}{r} \right)^6 \right]. \quad (3)$$

Here $\phi^{(A,B)}$ is the potential energy for two molecules *A* and *B* separated by a distance r ; the parameters $\sigma^{(A,B)}$, $\epsilon^{(A,B)}$ represent the collision diameter and depth of the energy well. The r^{-6} term describes attractive forces: the dispersion forces (London forces or induced-dipole–induced-dipole forces) (Israelachvili, 1991, p. 83). The r^{-12} contribution represents short-range repulsive forces. The corresponding expression for $\mathbf{f}^{(A,B)}$ is

$$\mathbf{f}^{(AB)} = -\nabla(n^{(A)}n^{(B)}\phi^{(A,B)}), \quad (4)$$

where $n^{(A)}$ and $n^{(B)}$ are the number densities at the specified points in phases *A* and *B*. For a gas, intermolecular forces attributable to a Lennard–Jones potential are pairwise additive (Hirschfelder et al., 1954, p. 148).

2.2. Estimating $\mathbf{b}^{(f,\text{corr})}$

In the following section, we will use Eq. (3) to find the density distribution in a supercritical fluid *f* within the immediate neighborhood of a crystalline solid *s*. We will find

shortly that we will require $\mathbf{b}^{(f,\text{corr})}$, the correction for intermolecular forces at any point in the supercritical fluid attributable to the presence of the crystalline solid.

From Eqs. (2) and (4), at each point in the gas or fluid phase

$$\begin{aligned} \mathbf{b}^{(f,\text{corr})} &= n^{(f)} \left[- \int_{R^{(s)}} \nabla(n^{(s)}\phi^{(f,s)}) dV \right. \\ &\quad \left. + \int_{R^{(s)}} \nabla(n^{(f,\text{bulk})}\phi^{(f,f)}) dV \right] \\ &= -n^{(f)} \left[\nabla \int_{R^{(s)}} n^{(s)}\phi^{(f,s)} dV \right. \\ &\quad \left. - \nabla \int_{R^{(s)}} n^{(f,\text{bulk})}\phi^{(f,f)} dV \right] \\ &= -n^{(f)} \nabla \Phi^{(f,\text{corr})}. \end{aligned} \quad (5)$$

Here

$$\Phi^{(f,\text{corr})} \equiv \int_{R^{(s)}} n^{(s)}\phi^{(f,s)} dV - \int_{R^{(s)}} n^{(f,\text{bulk})}\phi^{(f,f)} dV \quad (6)$$

and $n^{(f,\text{bulk})}$ is the number density in the fluid that would exist, if the solid were not present.

In discussing the intermolecular forces between a gas and a crystalline solid such as graphite, Steele (1973, 1974, 1978) assumed that the Lennard–Jones potential was also applicable. He recognized that pairwise additivity of intermolecular forces could be expected to be in error, but he argued that he “at least partially by-passed this problem by using semi-empirical pair-wise potentials that are reasonably closely related to the bulk properties” of the crystalline solid (Steele, 1974, p. 52). For this reason, he assumed that the crystalline solid was not continuously distributed in space, but instead discretely distributed in a layered lattice, each layer being laterally continuous. As a result, Steele (1974, 1978) computed

$$\begin{aligned} \int_{R^{(s)}} n^{(s)}\phi^{(f,s)} dV &= \frac{2\pi n_c \sigma^{(f,s)^2} \epsilon^{(f,s)}}{a_c} \left\{ \frac{2}{5} \left[\left(\frac{\sigma^{(f,s)}}{z} \right)^{10} \right. \right. \\ &\quad \left. \left. + \frac{\sigma^{(f,s)^{10}}}{9\Delta(z+0.72\Delta)^9} \right] \right. \\ &\quad \left. - \left(\frac{\sigma^{(f,s)}}{z} \right)^4 - \frac{\sigma^{(f,s)^4}}{3\Delta(z+0.61\Delta)^3} \right\}. \end{aligned} \quad (7)$$

Here z is the coordinate measured into the fluid *f*, perpendicular to the lattice planes (and therefore perpendicular to the surface) of the solid *s*; $z = 0$ can be interpreted either as the surface of the solid or as the center of the atoms in the first lattice plane. The Lennard–Jones parameters $\epsilon^{(f,s)}$ and $\sigma^{(f,s)}$ between fluid and solid are taken from (Steele, 1974, p. 56), n_c is the number of atoms in the unit surface cell, Δ is the distance between lattice planes, a_c is the area of the unit cell in the lattice plane. The number density for the solid $n^{(s)} = n_c/(a_c\Delta)$. We will use the values of $n^{(s)}$ and

Δ given by Tan and Gubbins (1990). To our knowledge, Steele's argument justifying the use of additivity has never been tested. We will say more about this in Section 4.

Similarly, we find

$$\int_{R^{(s)}} n^{(f,\text{bulk})} \phi^{(f,f)} dV = - \frac{4\pi n^{(f,\text{bulk})} \varepsilon^{(f,f)} (\sigma^{(f,f)})^{12}}{45z^9} + \frac{4\pi n^{(f,\text{bulk})} \varepsilon^{(f,f)} (\sigma^{(f,f)})^6}{6z^3} \quad (8)$$

in which $n^{(f,\text{bulk})}$ is the number density of the fluid that would be observed in the absence of the solid; $\varepsilon^{(f,f)}$ and $\sigma^{(f,f)}$ are the Lennard–Jones parameters for the fluid given by Bird et al. (2002, p. 864).

3. Density distribution

In one dimension, with the help of Eq. (5) and the chain rule, Eq. (1) becomes

$$\frac{1}{c^{(f)}} \left(\frac{dP^{(f)}}{dc^{(f)}} \right)_T \frac{dc^{(f)}}{dz} + N \frac{d\Phi^{(f,\text{corr})}}{dz} = 0. \quad (9)$$

Here $(dP^{(f)}/dc^{(f)})_T$ will be evaluated using an empirical equations of state for argon (Michels, et al., 1949), for krypton (Trappeniers et al., 1966), and for methane (Trappeniers et al., 1979, 1980); N is Avogadro's number; $c^{(f)} = n^{(f)}/N$ is the molar density in the interfacial region. The solution of this differential equation with the boundary condition

$$\text{as } z \rightarrow \infty : c^{(f)} \rightarrow c^{(f,\text{bulk})} \quad (10)$$

gives a density distribution.

The surface excess or the apparent adsorption

$$\Gamma^{(\sigma)} \equiv \int_{\delta}^{\infty} (c^{(f)} - c^{(f,\text{bulk})}) dz. \quad (11)$$

Since δ is not a known parameter, it must be defined. From Eqs. (6) and (9), there are two values of z at which $\Phi^{(f,\text{corr})} = 0$ and $c^{(f)} = c^{(f,\text{bulk})}$. One is as $z \rightarrow \infty$; the other we will define to be $z = \delta$. The graphite is assumed to be impermeable to the fluid.

4. Comparison with experimental data

Before comparing Eq. (11) with experimental data, let us consider the sources of experimental error. For graphitized carbon blacks, the uncertainty in the measured surface area is approximately 10% (Specovius and Findenegg, 1978; Steele, 1974), which translates to 10% uncertainty in the surface excess mass. Specovius and Findenegg (1978) and Blumel et al. (1982) found the maximum relative error in their buoyancy correction to be 3% and 4%, respectively, the values of which could be expected to increase as the critical point was approached. Other errors such as base-line drift were reported to be < 1%. Precluding any random or systematic error, the uncertainty of the results should be less than 15%.

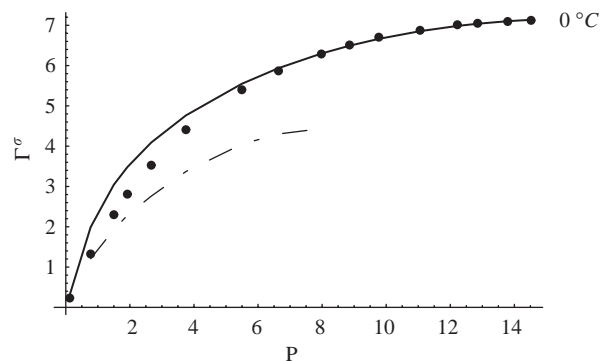


Fig. 3. Γ^{σ} ($\mu\text{mol}/\text{m}^2$) as a function of P (MPa) for argon on Graphon at 0°C predicted by Eq. (11) (the solid curve). The experimental observations are from Specovius and Findenegg (1978). The dashed-dot curve represents the computations of Sokolowski (1982).

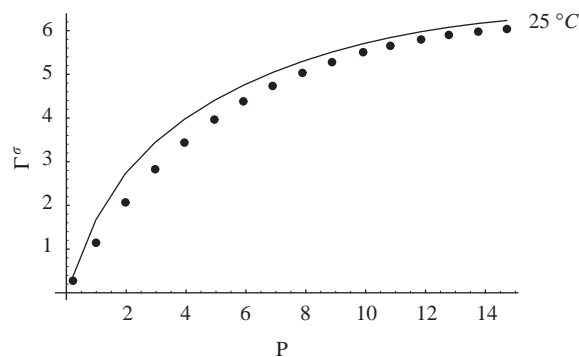


Fig. 4. Γ^{σ} ($\mu\text{mol}/\text{m}^2$) as a function of P (MPa) for argon on Graphon at 25°C predicted by Eq. (11) (the solid curve). The experimental observations are from Specovius and Findenegg (1978).

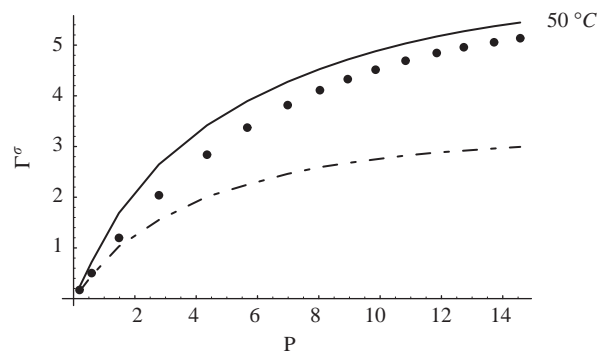


Fig. 5. Γ^{σ} ($\mu\text{mol}/\text{m}^2$) as a function of P (MPa) for argon on Graphon at 50°C predicted by Eq. (11) (the solid curve). The experimental observations are from Specovius and Findenegg (1978). The dashed-dot curve represents the computations of Fischer (1978).

In the comparisons of Eq. (11) with the experimental data in Figs. 3–12, we would like to emphasize that no adjustable parameters have been used. Eq. (11) describes these data within the uncertainty range for argon and krypton as well as for methane at 50°C .

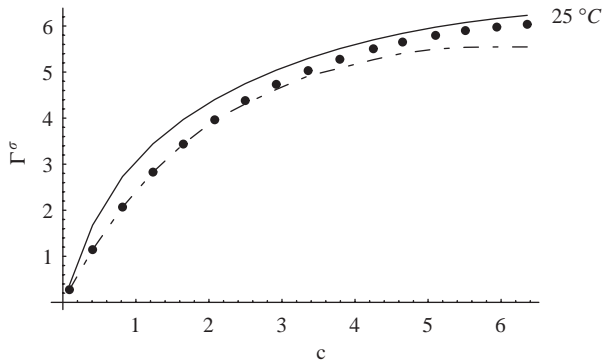


Fig. 6. Γ^σ ($\mu\text{mol}/\text{m}^2$) as a function of c (mol l^{-1}) for argon on Graphon at 25°C predicted by Eq. (11) (the solid curve). The experimental observations are from Specovius and Findeneegg (1978). The dashed line represents the computations of Egorov (2001).

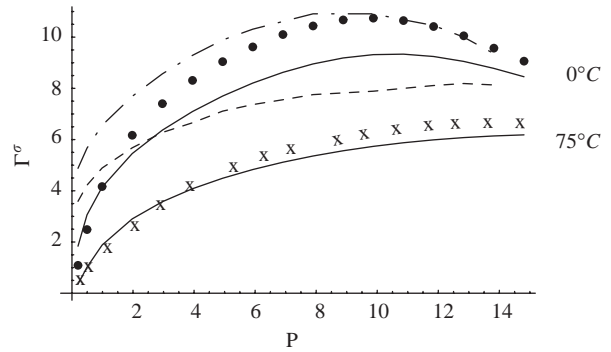


Fig. 9. Γ^σ ($\mu\text{mol}/\text{m}^2$) as a function of P (MPa) for krypton on Graphon at 0°C and at 75°C predicted by Eq. (11) (the solid curves). The experimental observations are from Blumel et al. (1982). The dashed-dot curve represents the computations of Rangarajan et al. (1995) for 0°C , the dashed curve for 75°C .

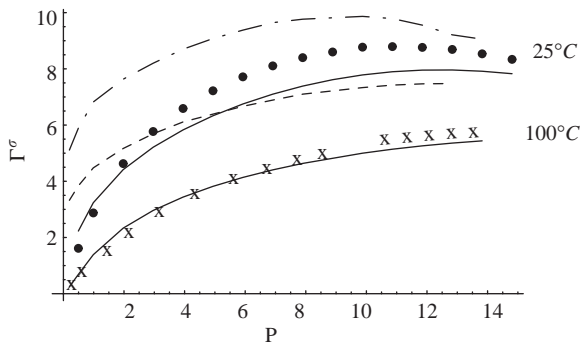


Fig. 7. Γ^σ ($\mu\text{mol}/\text{m}^2$) as a function of P (MPa) for krypton on Graphon at 25°C and at 100°C predicted by Eq. (11) (the solid curves). The experimental observations are from Blumel et al. (1982). The dashed-dot curve represents the computations of Rangarajan et al. (1995) for 25°C , the dashed curve for 100°C .

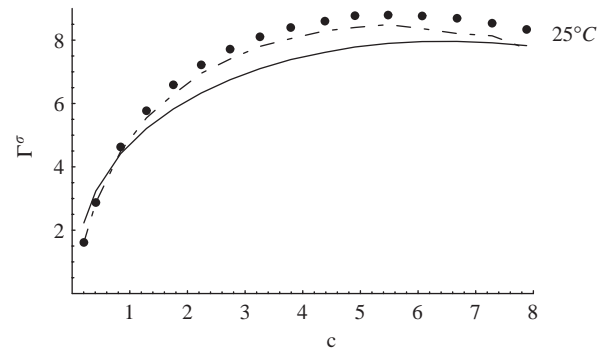


Fig. 10. Γ^σ ($\mu\text{mol}/\text{m}^2$) as a function of c (mol l^{-1}) for krypton on Graphon at 25°C predicted by Eq. (11) (the solid curves). The experimental observations are from Blumel et al. (1982). The dashed curve represents the computations of Egorov (2001).

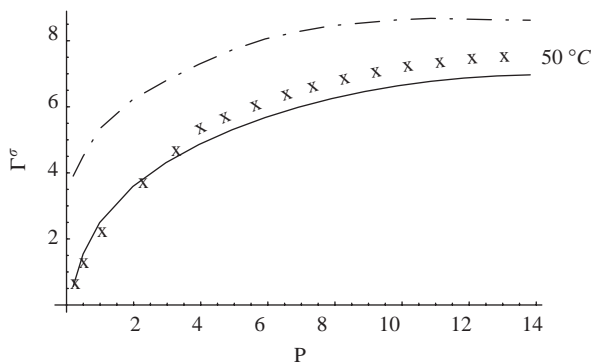


Fig. 8. Γ^σ ($\mu\text{mol}/\text{m}^2$) as a function of P (MPa) for krypton on Graphon at 50°C predicted by Eq. (11) (the solid curves). The experimental observations are from Blumel et al. (1982). The dashed-dot curve represents the computations of Rangarajan et al. (1995).

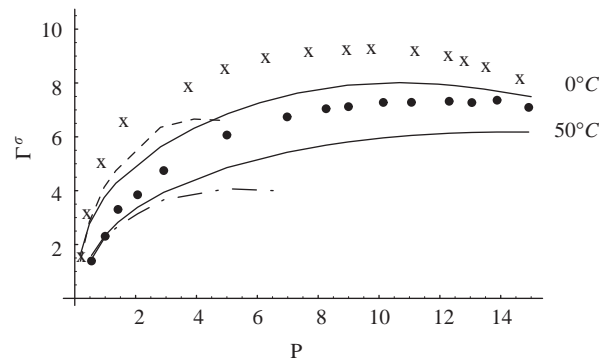


Fig. 11. Γ^σ ($\mu\text{mol}/\text{m}^2$) as a function of P (MPa) for methane on Graphon at 0°C and at 50°C predicted by Eq. (11) (the solid curves). The experimental observations are from Specovius and Findeneegg (1978). The dashed curve represents the computations of Sokolowski (1982) for 0°C , the dashed-dot curve for 50°C .

It is clear that, for both krypton and for methane, Eq. (11) underestimates the data, the error becoming progressively larger as the temperature decreases. There are at least two possible explanations.

As noted earlier in Section 2.2, Steele (1974, p. 52) expressed some doubt about the assumption of additivity of intermolecular forces in using his semi-empirical extension of the Lennard–Jones potential to the interactions between

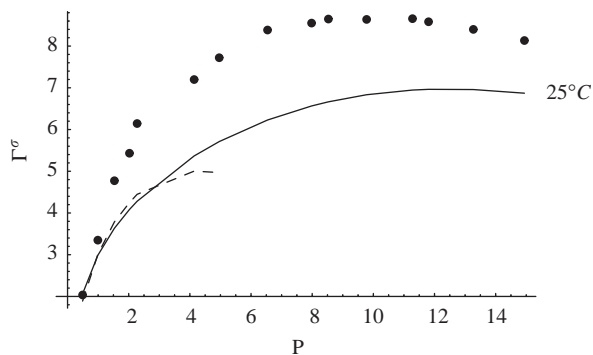


Fig. 12. Γ^σ ($\mu\text{mol}/\text{m}^2$) as a function of P (MPa) for methane on Graphon at 25°C predicted by Eq. (11) (the solid curves). The experimental observations are from Specovius and Findenegg (1978). The dashed curve represents the computations of Sokolowski (1982).

a crystalline solid and a gas. He proposed that this problem could be at least partially avoided by using a more realistic description of the solid. For this reason, he described the solid as being discretely rather than continuously distributed in space. While this proposal has not been previously tested experimentally to our knowledge, we believe that the excellent agreement between the predictions of our theory and the experimental observations for argon does support the use of pairwise additivity, at least when the temperature is sufficiently above the critical temperature T_c . Notice that for argon $T_c = 150.8$ K. For krypton, $T_c = 209.4$ K, and we have excellent agreement between our predictions and the experimental observations at 100°C , but errors increase as the temperature decreases, the density increases, and the interference of neighbors of krypton increases. In summary, we believe that pairwise additivity can be used as suggested by Steele (1974, p. 52), as long as the temperature is sufficiently above the critical temperature.

The poor agreement between our predictions and the experimental observations for methane is due in part to the same failure of pairwise additivity as the critical temperature $T_c = 190.4$ K is approached. But the errors are larger than those seen with krypton, which has a higher T_c . We do see the errors decrease as the temperature is raised, but we do not have measurements at high temperatures. However, we are also concerned that the Lennard–Jones potential may not be appropriate, particularly in denser fluids, because the methane molecule is not spherical.

5. Comparison with previous theories

As mentioned in the introduction, there are four analyses based upon statistical mechanics which have been compared with these same data: Egorov (2001), Rangarajan et al. (1995), Sokolowski (1982), and Fischer (1978). In all cases, we have used the results from their figures without repeating their computations.

Fig. 6 compares the computations of Egorov (2001) with Eq. (11) for the argon data of Specovius and Findenegg (1978) at 25°C ; Fig. 10 compares the two theories for the krypton data of Blumel et al. (1982). The computations of Egorov (2001) are excellent, although, as he notes, they begin to fail at higher densities. Unfortunately, he did not report computations for higher temperatures.

Figs. 7–9 compare the model of Rangarajan et al. (1995) with (11) for the krypton data of Blumel et al. (1982). Figs. 3, 11, and 12 compare the Sokolowski (1982) model with both Eq. (11) and the argon and methane data of Specovius and Findenegg (1978). Fischer (1978) presented a plot of his results compared with the data of Specovius and Findenegg (1978) for argon at only one temperature, 50°C . Fig. 5 compares his results with Eq. (11). In all cases Eq. (11) was superior.

6. Conclusions

The purpose of this paper is to present the first application of a new extension of continuum mechanics to the nanoscale (not the molecular scale) in which a correction for intermolecular forces from the adjoining phase is introduced in the differential momentum balance. We feel that we have successfully demonstrated this theory for supercritical adsorption of argon on Graphon (a graphitized carbon black) using no adjustable parameters.

Our theory does not do as well in describing the supercritical adsorption of krypton or of methane as the critical point is approached. We do not feel that this indicates a failure or limitation of the theory, but rather a limitation in the way that the theory was executed. Following Steele (1973, 1974, 1978), we have assumed the Lennard–Jones potential can be used to describe the carbon–fluid as well as the fluid–fluid interactions, and we have assumed that long-range intermolecular forces are pairwise additive.

We believe that the poorer agreement between our predictions and the experimental observations for krypton at lower temperatures is attributable to the assumption of pairwise additivity beginning to fail. The critical temperature for argon $T_c = 150.8$ K; for krypton, $T_c = 209.4$ K. Since the assumption of pairwise additivity would begin to fail as $T \rightarrow T_c$ and the fluid became denser, we could expect to see these effects at higher temperatures with krypton than with argon.

The poor agreement between our predictions and experimental observations for methane is certainly due in large measure to this same failure of the assumption of pairwise additivity. For methane, $T_c = 190.4$ K, and the error in our predictions decreases as the temperature is increased. However, we are also concerned that the Lennard–Jones potential may not be appropriate, particularly in the denser fluids as T_c is approached, because the methane molecule is not spherical.

Steele (1974, p. 52) clearly recognized that pairwise additivity of intermolecular forces could not be justified in condensed materials. He proposed that this problem could be at least partially avoided by using a more realistic description of the solid, one in which the crystalline solid was distributed discretely rather than continuously in space. We believe that the excellent agreement between the predictions of our theory and the experimental observations for argon and krypton, particularly at higher temperatures, supports his proposal.

We wish to emphasize that the use of pairwise additivity is not an inherent limitation in the use of this theory. For example, in describing the interactions between two condensed media, the limitations of pairwise additivity can be avoided by describing the two-point interactions using an effective, Lifshitz type, Hamaker constant that is both screened and retarded (Bowen and Jenner, 1995).

Notation

a_c	area of unit cell on the lattice plane
$\mathbf{b}^{(A, \text{corr})}$	body force correction for intermolecular forces per unit volume, defined by Eq. (2)
$c^{(f)}$	molar density of supercritical fluid, equal to $n^{(f)}/N$
$c^{(f, \text{bulk})}$	molar density of supercritical fluid that would exist in the absence of the crystalline solid
dV	indicates that a volume integration is to be performed
$\mathbf{f}^{(A, B)}$	force per unit volume of phase A per unit volume of phase B
$n^{(A)}$	number density at the specified point in phase A
$n^{(A, \text{bulk})}$	number density that would exist in phase A , if phase B were not present
n_c	number of atoms in the unit cell on the lattice plane
N	Avogadro's number
$P^{(A)}$	Thermodynamic pressure of fluid phase A
r	separation distance in Lennard–Jones potential (3)
$R^{(B)}$	region occupied by phase B
T_c	critical temperature
z	coordinate measured into the fluid, normal to the lattice plane (and therefore perpendicular to the surface); $z = 0$ can be interpreted either as the surface of the solid or as the center of the atoms in the first lattice plane.

Greek letters

$\Gamma^{(\sigma)}$	surface excess mmoles per unit area defined by Eq. (11)
δ	value of z at which $c^{(f)} = c^{(f, \text{bulk})}$; see also discussion following Eq. (11)
Δ	distance between lattice planes

$\varepsilon^{(AB)}$	Lennard–Jones well depth in Eq. (3)
$\sigma^{(AB)}$	Lennard–Jones collision diameter in Eq. (3)
$\phi^{(AB)}$	Lennard–Jones potential defined by Eq. (3)
$\Phi_{(f, \text{corr})}$	defined by Eq. (6)

Acknowledgements

The authors appreciate the help given by Eun-Suok Oh in using Mathematica (Wolfram research 1999).

References

- Abraham, F.F., Singh, Y., 1978. Comment on “the structure of a hard sphere fluid in contact with a soft repulsive wall”. *Journal of Chemical Physics* 68, 4767–4768.
- Aranovich, G.L., Donohue, M.D., 1996. Adsorption of supercritical fluids. *Journal of Colloid and Interface Science* 180, 537–541.
- Bird, R.B., Stewart, W.E., Lightfoot, E.N., 2002. *Transport Phenomena*, 2nd Edition. Wiley, New York.
- Blumel, S., Koster, F., Findenegg, G.H., 1982. Physical adsorption of krypton on graphite over a wide density range. *Journal of the Chemical Society-Faraday Transactions 2* 78, 1753–1764.
- Bowen, W.R., Jenner, F., 1995. The calculation of dispersion forces for engineering applications. *Advances in Colloid and Interface Science* 56, 201–243.
- Cao, D., Wang, W., Duan, X., 2002. Grand canonical monte carlo simulation for determination of optimum parameters for adsorption of supercritical methane in pillared layered pores. *Journal of Colloid and Interface Science* 254, 1–7.
- Egorov, S.A., 2001. Adsorption of supercritical fluids and fluid mixtures: inhomogeneous integral equation study. *Journal of Physical Chemistry B* 105, 6583–6591.
- Findenegg, G.H., Fischer, J., 1975. Adsorption of fluids: simple theories for the density profile in a fluid near an adsorbing surface. *Faraday Discussions of the Chemical Society* 59, 38–45.
- Fischer, J., 1977. Three-dimensional virial expansions in physical adsorption. *Molecular Physics* 34, 1237–1245.
- Fischer, J., 1978. Physical adsorption at high pressures and high temperatures: the density profile of the gas. *Journal of Chemical Physics* 68, 3947–3948.
- Gusev, V.Y., O'Brien, J.A., Seaton, N.A., 1997. A self-consistent method for characterization of activated carbons using supercritical adsorption and grand canonical monte carlo simulations. *Langmuir* 13 (10), 2815–2821.
- Hirschfelder, J.O., Curtiss, C., Bird, R.B., 1954. *Molecular Theory of Gases and Liquids*. Wiley, New York. corrected with notes added 1964.
- Israelachvili, J.N., 1991. *Intermolecular and Surface Forces*, 2nd Edition. Academic Press, New York.
- Lozano-Castelló, D., Cazorla-Amorós, D., Linares-Solano, A., Quinn, D.F., 2002. Micropore size distributions of activated carbons and carbon molecular sieves assessed by high-pressure methane and carbon dioxide adsorption isotherms. *Journal of Physical Chemistry B* 106, 9372–9379.
- Michels, A., Wijker, H., Wijker, H., 1949. Isotherms of argon between 0°C and 150°C and pressures up to 2900 atmospheres. *Physica* 7, 627–633.
- Miyawaki, J., Kanda, T., Suzuki, T., Okui, T., Maeda, Y., Kaneko, K., 1998. Macroscopic evidence of enhanced formation of methane nanohydrates in hydrophobic nanospaces. *Journal of Physical Chemistry B* 102, 2187–2192.

- Murata, K., Kaneko, K., 2001. The general equation of supercritical gas adsorption isotherm. *Journal of Physical Chemistry B* 105, 8498–8503.
- Neimark, A.V., Ravikovitch, P.I., 1997. Calibration of pore volume in adsorption experiments and theoretical models. *Langmuir* 13 (19), 5148–5160.
- Ohkubo, T., Miyawaki, J., Kaneko, K., Ryoo, R., Seaton, N.A., 2002. Adsorption properties of templated mesoporous carbon (cmk-1) for nitrogen and supercritical methane—experiment and gcmc simulation. *Journal of Physical Chemistry B* 106, 6523–6528.
- Ono, S., Kondo, S., 1960. Molecular theory of surface tension in liquids. In: Flügge, S. (Ed.), *Encyclopedia of Physics, Structure of Liquids*, Vol. 10. Springer, Berlin, pp. 134.
- Rangarajan, B., Lira, C.T., Subramanian, R., 1995. Simplified local density model for adsorption over large pressure ranges. *A.I.Ch.E. Journal* 41, 838–845.
- Slattery, J.C., 1990. *Interfacial Transport Phenomena*. Springer, New York.
- Slattery, J.C., 1999. *Advanced Transport Phenomena*. Cambridge University Press, Cambridge.
- Sokolowski, S., 1982. Quantitative description of the adsorption of gases on graphite at high temperatures. *Journal of the Chemical Society-Faraday Transactions* 2 78, 255–264.
- Specovius, J., Findenegg, G.H., 1978. Physical adsorption of gases at high pressures: Argon and methane onto graphitized carbon black. *Berichte der Bunsengesellschaft fuer Physikalische Chemie* 82, 174–180.
- Steele, W.A., 1973. The physical interaction of gases with crystalline solids. *Surface Science* 36, 317–352.
- Steele, W.A., 1974. *The Interaction of Gases with Solid Surfaces*. Pergamon Press, New York.
- Steele, W.A., 1978. The interaction of rare gas atoms with graphitized carbon black. *Journal of Physical Chemistry* 82, 817–821.
- Tan, Z., Gubbins, K.E., 1990. Adsorption in carbon micropores at supercritical temperatures. *Journal of Physical Chemistry* 94, 6061–6069.
- Trappeniers, N.J., Wassenaar, T., Wolkers, G.J., 1966. Isotherms and thermodynamic properties of krypton at temperatures between 0°C and 150°C and at densities up to 620 amagat. *Physica* 32, 1503–1520.
- Trappeniers, N.J., Wassenaar, T., Abels, J.C., 1979. Isotherms and thermodynamic properties of methane at temperatures between 0°C and 150°C and at densities up to 570 amagat. *Physica A* 98, 289–297.
- Trappeniers, N.J., Wassenaar, T., Abels, J.C., 1980. Erratum isotherms and thermodynamic properties of methane at temperatures between 0°C and 150°C and at densities up to 570 amagat. *Physica A* 100, 660.
- Truesdell, C., Toupin, R.A., 1960. The classical field theories. In: Flügge, S. (Ed.), *Handbuch der Physik*, Vol. 3/1. Springer, Berlin, pp. 226–793.
- Zhou, L., Zhou, Y., Li, M., Chen, P., Wang, Y., 2000. Experimental and modeling study of the adsorption of supercritical methane on a high surface activated carbon. *Langmuir* 16, 5955–5959.